Nordic Hydrology, 28, 1997, 51-64

Characterization of Flood Waves by Rating Curves

S.K. Mishra, M.K. Jain, and S.M. Seth
National Institute of Hydrology, Roorkee-247 667 (U.P.), India

The flood waves are characterized within the frame-work of loop (or hysteresis) of rating curves. The National Weather Service's Dam Break Flood Forecasting Model is used to generate the flood waves in the downstream valley of the Bargi dam located in Central India. The quantified hystereses, η, of non-dimensional rating curves are related with the corresponding flood wave characteristics, *viz.*, speed of travel, wave number, phase difference, and attenuation. The analysis has led to the development of an exact relationship between η and phase difference. Using the concept of wave zoning, the better performance of the hysteresis based criteria compared with the available criteria is verified using Convex and Muskingum-Cunge routing in the wave zones. η limits are specified for the applicability of these simplified routing models. Furthermore, the envisaged applications of the based analysis are introduced.

Introduction

The approximate solutions of the non-linear St. Venant (SV) equations have provided a great insight to the flow phenomena in open channels. Ponce and Simons (1977) derived the shallow wave spectrum for the celerity and diffusion characteristics of the long waves using linear theory, and developed criteria for the identification of kinematic wave (KW) and diffusion wave (DW) (Ponce *et al.* 1978). The physical mechanism for the occurrence of these waves was explained by Menendez and Norshini (1982). Daluz Viera (1983) defined the regions of validity of these models using kinematic wave number and Froude number. Fread (1985) developed

criteria for defining the range of application of these models. Ponce (1989) recommended the use of Convex model and Muskingum-Cunge model for the identification and routing of KW and DW, respectively. Ponce *et al.* (1996) confirmed the applicability of Constant Parameter Muskingum-Cunge (CPMC) model to routing DWs. The importance of these simplified models, Convex and CPMC models, with respect to real world routing applications was advocated by Perumal (1994a).

The flood waves have also been characterized within the frame-work of loop (or hysteresis (NWS 1981; Kabir and Orsborn 1984) rating curves (Henderson 1966; French 1985). The attenuation characteristics were explained by Ponce (1989) and illustrated by Perumal (1994b). Recently, Mishra and Seth (1996) defined the flood wave characteristics in natural channels using quantified hysteresis, η, and developed criteria for the identification of KW, DW and dynamic wave (DYW). They also explained the physical significance of hysteresis by relating it with the channel and flow characteristics and energy loss. Mistry *et al.* (1984) found unsteadiness a major cause of hysteresis. Their finding was intuitively based on the observations on seven flood events on different streams of Gujarat (India). The general notion however is that the hysteresis is a manifestation of storage in the channel and is attributed to the secondary terms of SV's momentum equation (Ponce 1989; French 1985).

The numerical solution of the SV equations embodies numerical diffusion and numerical dispersion that are characterized by amplitude and phase error portraits (Leendertse 1967; Cunge 1969; Ponce *et al.* 1979; Ponce 1991). The National Weather Service's Dam Break Flood Forecasting (NWS DAMBRK) Model uses a weighted four-point finite difference implicit scheme for the solution of the SV equations due to stability, convergence and other reasons. Since the dam break flood encompasses the whole dynamic range of the waves and its nature changes from DYW to DW or KW as it travels downstream (Fread 1985), the dam break analysis of the Bargi dam located in Central India was considered for generating flood waves in the downstream valley of the dam using NWS DAMBRK Model. These waves have been characterized within the frame-work of non-dimensional hysteresis of site-specific rating curves and verified by Constant Parameter Convex (CPC) and CPMC routing in the portrayed wave zones. The verification, in turn, leads to the development η of criteria for the applicability of these simplified routing models.

Dam Break Study

The Bargi Dam, 59 m in height, is located in the Upper Narmada region falling in Central India(latitude 22°56'30" and longitude 79°55'30"). It is a major dam having a gross capacity of 5.06 billion cubic metre at maximum water level, 424.28 m, and it drains a catchment area of 14,555 km^2. The dam break analysis was carried out using NWS DAMBRK Model assuming gradual failure and following the guide-lines

laid down in the NWS DAMBRK Manual (1981). Seven cross-sections were available between the dam site and Punasa, and the other cross-sections used in the analysis were linearly interpolated. The presented results cover the 508 km reach between Jamtara (about 15 km downstream of the dam site) and Punasa.

Definitions

Hysteresis η

The hysteresis, η, is an index that measures the size (or area) of the loop in a non-dimensional rating curve. Mishra and Seth (1996) described it as a crude index of energy expended by the flood wave at a site under consideration during its time period. For computational purpose, the stage and the discharge values are made non-dimensional as below

$$h = \frac{H - H_{min}}{H_{max} - H_{min}} \tag{1}$$

$$q = \frac{Q - Q_{min}}{Q_{max} - Q_{min}} \tag{2}$$

Where, h is the dimensionless stage; H_{max} is the maximum computed depth at a site of interest; H_{min} is the minimum computed depth at a site of interest; and H is the computed depth at a site of interest. Similarly, Q stands for discharge, and q for dimensionless discharge.

Speed of Travel *c*

The speed of travel (Price 1973; 1985) is described as below

$$c = \frac{\Delta x}{tt} \tag{3}$$

Where, c is the speed of travel in m/s; Δx is the reach length in m; and tt is the time of travel of the flood peak in second.

Phase Difference ϕ

It is computed as below (Mishra and Seth 1996)

$$\phi = \frac{2\pi}{T}(t_{ph} - t_{pQ}) \tag{4}$$

where, ϕ is the phase difference in radian; T is the time period in hr; t_{ph} is the time of rise of stage wave(hr); and t_{pQ} is the time of rise of discharge wave (hr).

Attenuation

The attenuation is described by logarithmic decrement as below

$$\delta = \frac{c\,T}{\Delta x}\,(\ln Q_j - \ln Q_{j+1}) \qquad (5)$$

where, δ is the logarithmic decrement in one period of wave travel (dimensionless); T is in seconds; Q_j and Q_{j+1} are the peak discharges (cumec) at successive locations j and $j+1$, respectively; and Δx is in m. Greater δ corresponds to greater attenuation and *vice versa*.

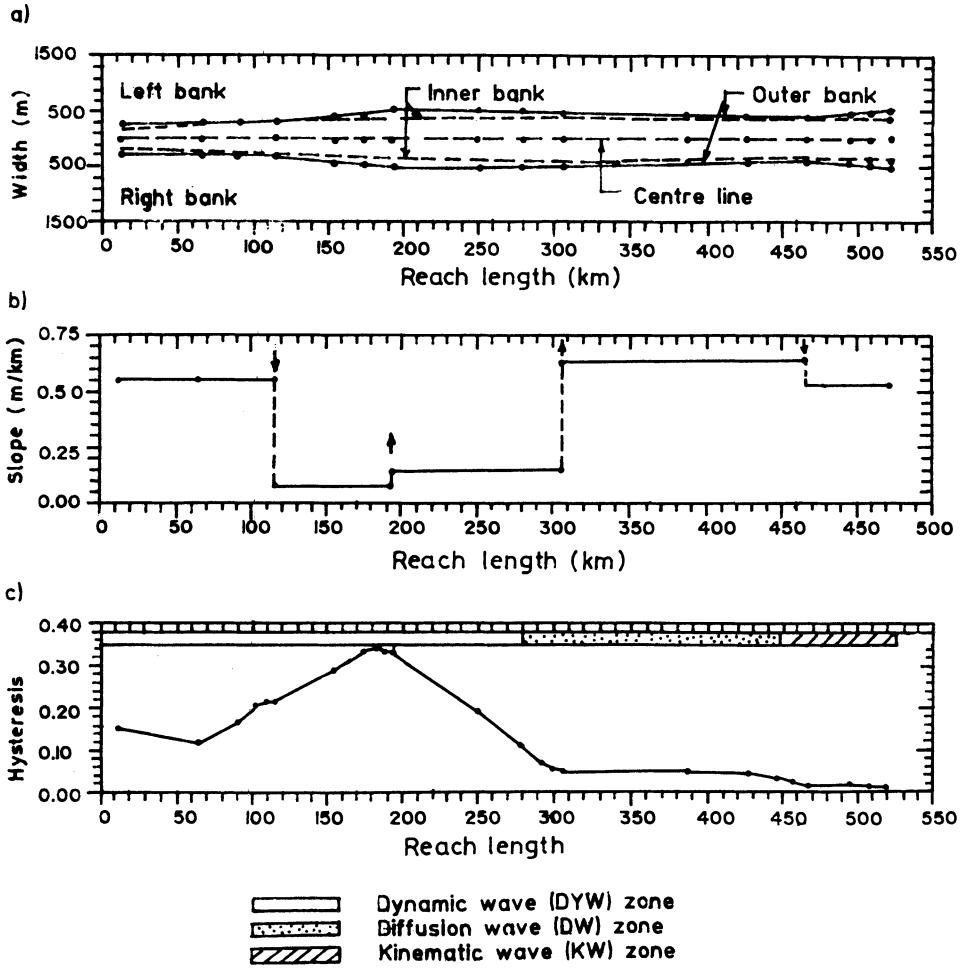

Fig.1. River reach characteristics (0 km corresponds to dam site):
(a) Plan view of river valley. The available cross-sections are presented by dots.
(b) Bed slope variation along the river valley. Up and down arrows marks indicate respectively steepening and flattening of adjoining downstream reaches.
(c) Hysteresis variation along the river valley.

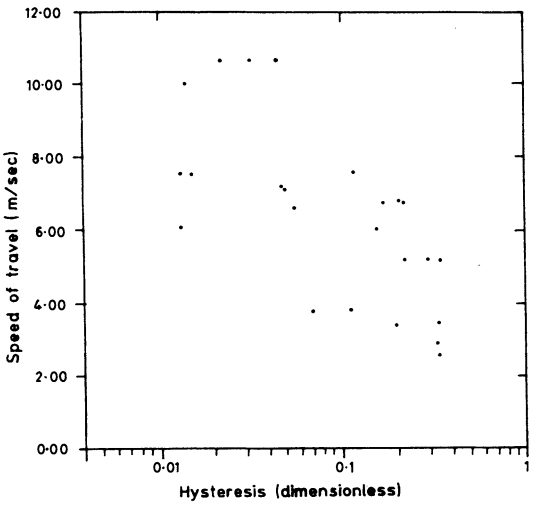

Fig.2. Dimensionless hysteresis *vs* speed of travel (m/s).

Relationship between η and Flood Wave Characteristics

Figs. 1(a), 1(b) and 1(c) show the plan view of the river reach, the slope variation along the reach, and the η variation, respectively. The slope of the river generally varies between $3x10^{-5}$ and $5x10^{-4}$ (Fig.1(b)). Its impact on the η variation is clearly reflected; where the slope is flatter (for example, in reach 115-307 km), the η values are higher than those where the slope is steeper (for example, in reach 307-465 km and adjacent downstream reach). Furthermore, where the slope changes from steeper to milder (for example, at 115 km), shown by down arrow marks, the η assumes a higher value than that where the slope changes from milder to steeper (for example, at 307 km), shown by up arrow marks. The channel is generally uniform (Fig.1(a)), and therefore, it has less impact on η variation than that of slope. It can be elicited that where the channel characteristics favour the energy loss, η values are higher in magnitude than those where the channel characteristics act otherwise.

Fig. 2 shows a plot between η and corresponding speed of travel, *c*. The aberrant nature of the data points is attributed to the interdependence between the speed and the attenuation of a flood wave (Price 1973; 1985). Eq. (3) does however not take the other into account. A generally decreasing trend (Eq. (6)) with increasing η can be obtained as follows

$$c = 3.445\ \eta^{-0.219} \qquad (6)$$

It leads to an interpretation that the less dynamic waves travel faster than the more dynamic waves do, or the waves travel faster on steeper slopes than they do on milder or flatter slopes.

To develop a relationship between η and the channel and flow characteristics the plots between η and corresponding $\hat{\sigma}$ (Fig. 3) and $\hat{\sigma}F_0$ values (Fig. 4) were drawn.

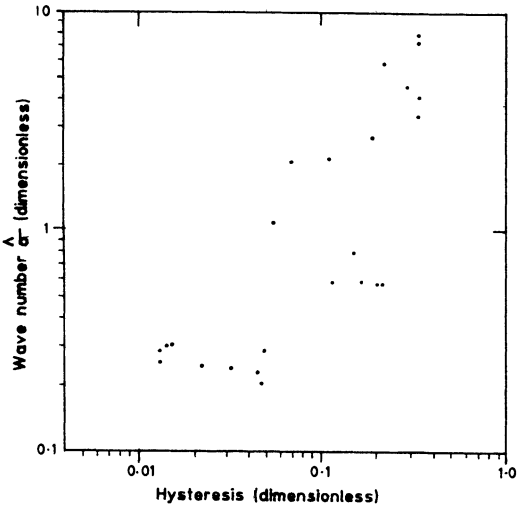

Fig.3. Dimensionless hysteresis *vs* dimensionless wave number, $\hat{\sigma}$.

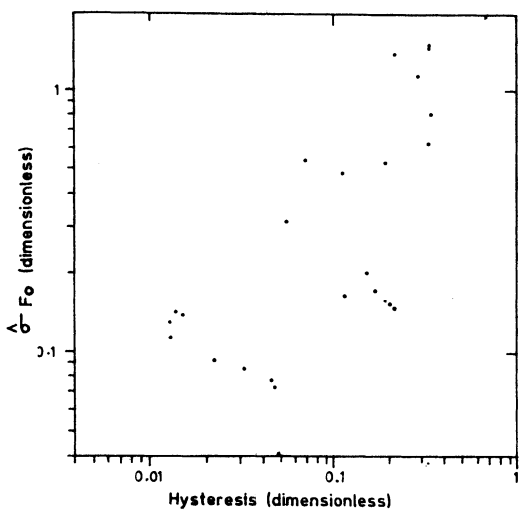

Fig.4. Dimensionless hysteresis *vs* dimensionless $\hat{\sigma}F_0$.

The following relationships were obtained

$$\eta = 0.085(\hat{\sigma})^{0.801} \tag{7}$$

$$\eta = 0.246(\hat{\sigma}F_0)^{0.841} \tag{8}$$

Where, $F_0(=u_0/\sqrt{gy_0}$; here, u_0 and y_0 are respectively the normal velocity and depth of flow; and g is the acceleration due to gravity); $\hat{\sigma}(=2\pi y_0/(LS_0))$ is the dimensionless wave number; L $(=cT)$ is the wave length; and S_0 is the bed slope. In Eqs. (7) and (8), F_0 is computed using u_{max} in place of u_0, and y_0 is replaced by hydraulic depth $(=A/B)$; where, B is the top width at H_{max}. For defining type of waves in natural channels the computed σ and $\hat{\sigma}F_0$ values corresponding to respective η limits

Table 1 – Criteria for wave types

Wave type	Hysteresis(h) (Dimensionless)	Phase Difference (f) (Radian)
Kinematic wave	$h < 0.025$	$f < 0.03$
Diffusion wave	$0.025 \leq h \leq 0.1$	$0.03 \leq f \leq 0.13$
Dynamic wave	$h > 0.1$	$f > 0.13$

Source: Mishra & Seth (1994; 1996)

given in Table 1 are 0.217 and 0.315, respectively. These values are however greater than those given by Eqs. (9) (for KW) and (10) (for DW) (Ponce *et al.* 1978), respectively

$$\frac{T_p S_0 u_0}{y_0} \geq 85 \quad \text{or} \quad \hat{\sigma} \leq 0.025 \tag{9}$$

$$T_p S_0 \left(\frac{q}{y_0}\right)^{\frac{1}{2}} \geq 15 \quad \text{or} \quad \hat{\sigma} F_0 \leq 0.140 \tag{10}$$

The wave is a DYW if it does not fall within the purview of KW and DW. Here, T_p is the time of rise of a flood wave assumed to be half of the wave period.

In an endeavour to show how the hysteresis of a particular loop rating curve of a site is related with the attenuating tendency of the discharge wave passing through that site, an exponential relation (Fig. 5) was developed as below

$$\delta = 0.048\, e^{10.6\,\eta} \tag{11}$$

Fig. 5 conforms to the established norms of attenuation of the waves with the kind of wave; as the wave changes from KW to DYW or η increases, the attenuation also increases. As $\eta \rightarrow 0$, the δ should also approach zero. The error in relationship (Eq. (11)) is however attributed to: a) the visual determination of the time period of the flood waves; and b) the errors involved in the celerity computations.

The plot between η and ϕ. (Fig. 6) gave the following linear relation (if both axes plotted to linear scale)

$$\phi = 1.531\,\eta - 0.005 \tag{12}$$

As both the axes of a dimensionless rating curve range 0-1, the η must range 0-1; η=0 corresponds to KW. Theoretically, ϕ=0 corresponds to either a KW or a Gravity Wave (GW), and $\phi=\pi$ corresponds to GW (Menendez and Norshini 1982). Therefore, from the works of Mishra and Seth (1994; 1996) and Eq. (12), the following exact relationship can be conveniently postulated

$$\phi = \frac{\pi}{2}\eta \tag{13}$$

Evidently, as $\eta \rightarrow 1.0$, $\phi \rightarrow \pi/2$. Eq. (13) does, however, not define the wave characteristics for ϕ values ranging between $\pi/2$ and π.

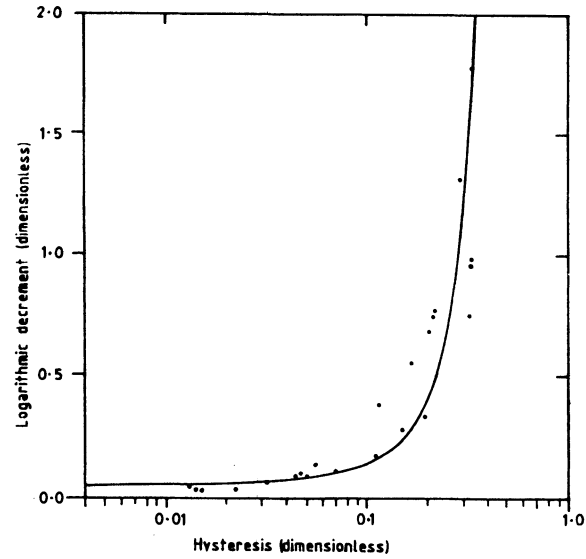

Fig.5. Dimensionless hysteresis *vs* dimensionless logarithmic decrement, d.

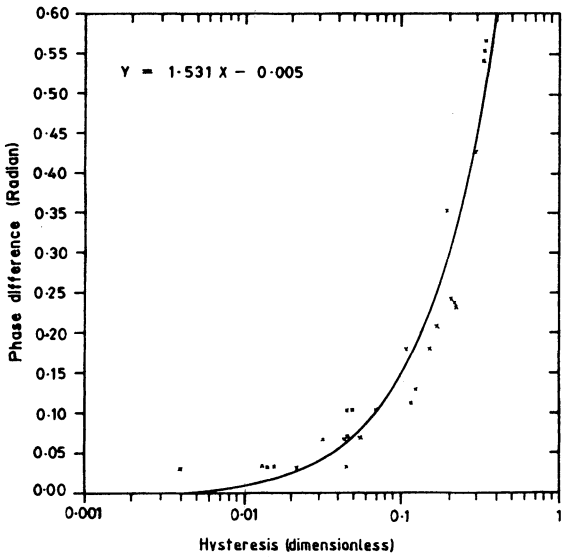

Fig.6. Dimensionless hysteresis *vs* phase difference, f (radian).

Table 2 – Comparative statement of wave types in different sub-reaches*

Criteria	Wave type		
	Kinematic	Diffusion	Dynamic
Ponce et al.(1978)	–	14-115 307-522	115-307
Hysteresis (Table 1)	451-522	282-451	14-282

* Sub-reach location in km.

Zoning of River Reach for Wave Types

Utilizing the inequalities (Eqs. (9) and (10)), the zones of different kinds of waves occurring along the river valley during the propagation of the dam break flood wave were identified (Table 2). The information on H_{max}, Q_{max} and T at different locations were used in characterizing a wave type at these locations. Table 2 reveals that the application of the inequality criteria (Eqs. (9) and (10)) to the sub-reaches 14-115 and 307-522 km results in a DW, and in the rest of the reach, the wave is described a DYW. However, the shaded zones (based on η criteria given in Table 1) in Fig. 1(c), also summarized in Table 2, indicate that the wave is a KW in the sub-reach 451-522 km, and in the sub-reach 282-451 km, it is a DW. In other parts of the reach, it is a DYW. Major inconsistencies arise in the sub-reaches 14-115, 281-307 and 451-522 km. In sub-reaches 14-115 and 281-307 km, the Ponce *et al.* criteria reveal DW and DYW, respectively and the η criteria, the DYW and DW, respectively. In the sub-reach 451-522 km the former criteria reveal DW and the latter, the KW. This discrepancy is sorted out by routing the flows in the sub-reaches by CPC and CPMC methods described in the following section.

Verification of Wave Types by CPC and CPMC Routing

To verify the wave types in the wave zones, shown in Fig. 1(c), routing was carried out in the DW and KW zones. The CPMC was applied to the sub-reaches in DW zone and the CPC method, to the sub-reaches in KW zone. To keep the Courant number ($=c\Delta t/\Delta s$; where c is in m/s; Δt is the time interval in second; and Δs is the

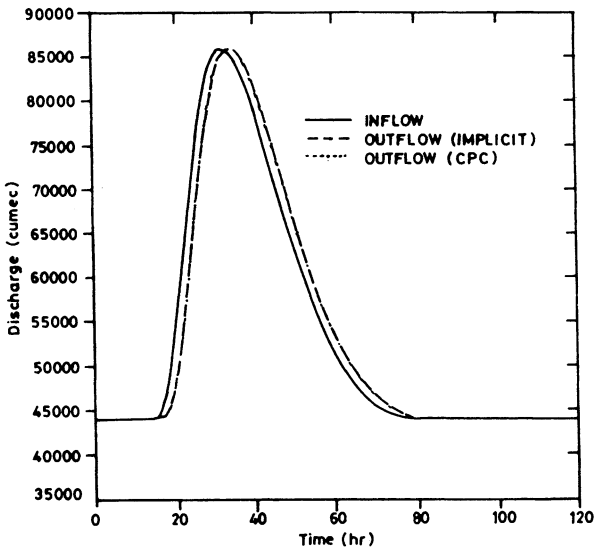

Fig.7. Simulation of outflow using Convex method for river reach 446-520 km.

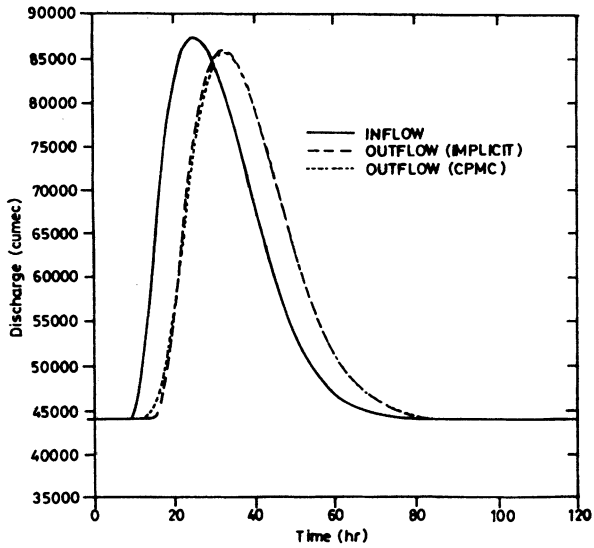

Fig.8. Simulation of outflow using Muskingum-Cunge method for river reach 278-446 km.

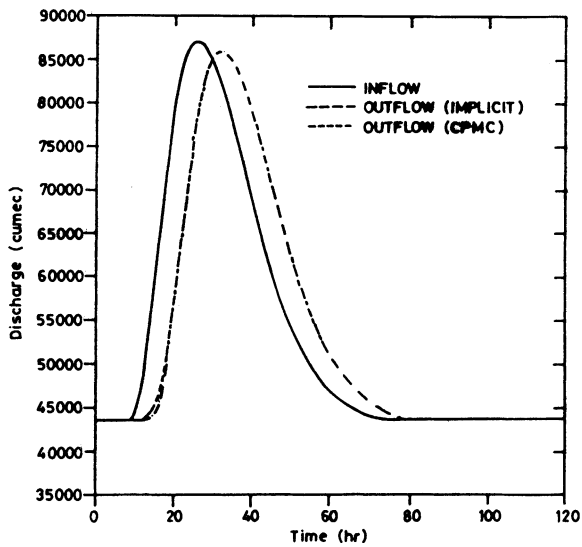

Fig.9. Simulation of outflow using Muskingum-Cunge method for river reach 293-446 km.

reach length in m) near 1.0 the sub-reaches were suitably sub-divided to avoid negative outflow problem (Ponce 1989).

The simulation results by CPC routing in the sub-reach, 446-520 km ($\eta < 0.025$ in Fig. 1c) are shown in Fig.7. Evidently, the excellent match with that due to the IMPLICIT scheme verifies the occurrence of KW in this sub-reach. The application re-

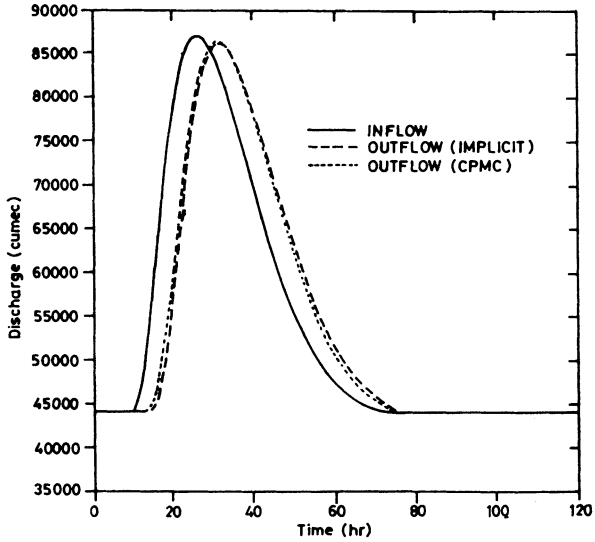

Fig.10. Simulation of outflow using Muskingum-Cunge method for river reach 300-446 km.

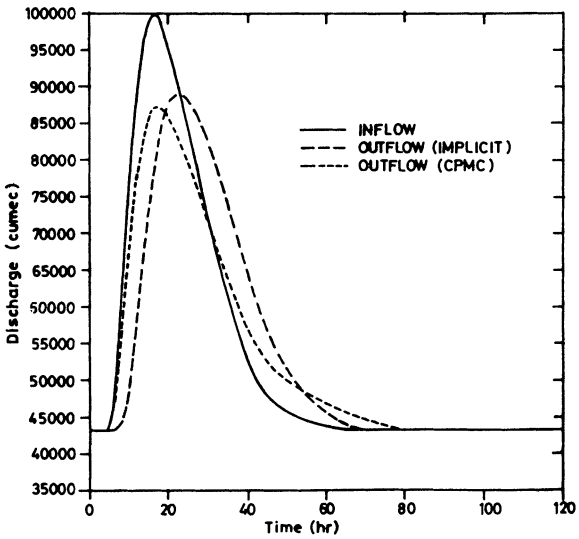

Fig.11. Simulation of outflow using Muskingum-Cunge method for river reach 183-250 km.

sults of CPMC method for the sub-reaches, 278-446, 293-446 and 300-446 km are depicted in Figs. 8-10, respectively. The remarkable simulation results underscore not only the verification of occurrence of DWs in these sub-reaches but also the applicability of CPMC method to these sub-reaches, where η values lie in the range 0.032-0.111. To test its applicability to the DYW sub-reaches (Fig. 1(c)) it was ap-

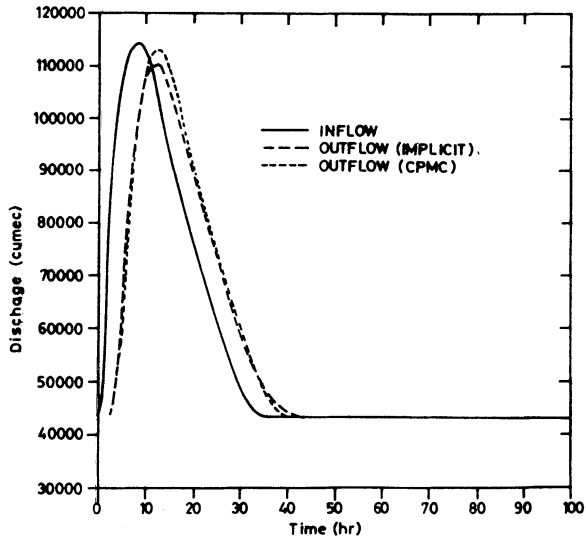

Fig.12. Simulation of outflow using Muskingum-Cunge method for river reach 14-102 km.

plied to the sub-reaches 183-250 and 14-102 km. Ostensibly, the CPMC method fails to simulate the flood peak (Figs. 11 and 12) as well as the time to peak (Fig. 11). In these sub-reaches, η values lie in the range 0.151-0.338, the range for DYW (Table 1).

Conclusion

The flood waves generated using NWS DAMBRK Model at various locations in the downstream valley of Bargi dam in Central India have been characterized by the non-dimensional hysteresis, η, of the developed site-specific rating curves. The flood wave characteristics, the speed of travel, the wave number, the attenuation, and the phase difference have been related with η. With the increase in η, the speed of travel generally decreases, the wave number increases, the attenuation shows an exponentially rising trend, and the phase difference shows a linearly rising trend. An exact relationship between η and the phase difference has also been drawn. These relationships confirm the dependence of these characteristics on η. The remarkable simulation of flows by CPC and CPMC routing in the KW and DW regions, defined by η criteria, respectively with those by IMPLICIT scheme not only confirms the occurrence of these waves in the specified η range but also underscores the applicability of CPC and CPMC in the specified wave regions.

Applications

The following applications of hysteresis based study are envisioned:

- The hysteresis based criteria can be used to determine wave type for application of suitable simplified routing models, *viz.* CPC and CPMC methods, to natural channels.
- The η criteria can be used to locate the fictitious downstream boundary – where the actual wave condition is consistent with the supplied boundary condition – for improving the NWS DAMBRK results.
- The exact relationship (Eq. (13)) can also be used to determine the time period, T, if the information on the other variables is available. It can help in base flow separation and, in turn, can be of use in unit hydrograph based analyses.
- This approach can be applied in processing the discharge hydrographs (derived using engineer's rating curve) for phase difference.

Acknowledgement

The authors sincerely acknowledge Professor Ian Cordery, School of Civil Engineering, the University of New South Wales, Sydney, Australia for his thoroughly going through the draft manuscript and providing valuable suggestions. The suggestions of anonymous reviewers are gratefully acknowledged.

References

Cunge, J.J. (1969) On the subject of a flood propagation computation method (Muskingum method), *J. Hydraul. Res., Vol. 7(2)*, pp. 205-230.

Daluz Viera, J.H. (1983) Conditions governing the use of approximations for the St. Venant equations for shallow water, *J. Hydrol., Vol. 60*, pp. 43-58.

Fahmy, H.E.S., and Morel-Seytoux, H.J. (1994) Hybrid non-inertia and statistical model versus hydrodynamic routing, *J. Hydraul. Engg., ASCE, Vol. 120(6)*, pp. 706-721.

Fread,D.L. (1985) Applicability criteria for kinematic and diffusion routing models, Lab. of Hydrology, National Weather Service, NOAA, U.S. Department of Commerce, Silver Spring, Maryland.

French, R.H. (1985) *Open channel hydraulics*, McGraw-Hill Book Co., Inc., New York, NY, pp. 551.

Henderson, F.M. (1966) *Open Channel Flow*, Macmillan Publishing Co., Inc., New York.

Kabir, N., and Orsborn, J.F. (1984) Numerical flood routing for natural channels, In: Proc. Water for Resources and Development Conf. (14-17 Aug., ASCE, New York, USA), ed. D.L. Schreiber, pp. 148-152.

Leendertse, J.J. (1967) Aspects of a computational model for long period water wave propagation, RM-5294-PR, The Rand Corporation, Santa Monica, California, USA.

Menéndez, A.N., and Norshini, R. (1982) Spectrum of shallow water waves: An analysis, *J. Hydr. Div., ASCE, Vol. 108 (HY1)*, pp. 75-94.

Mishra, S.K., and Seth, S.M. (1994) Effect of downstream boundary conditions on dam break flood wave propagation characteristics, Technical report, TR(BR) 117, National Institute of Hydrology, Roorkee (India).

Mishra, S.K., and Seth, S.M. (1996) Use of hysteresis for defining the nature of flood wave propagation in natural channels, *Hydrological Sciences-Journal-des Sciences Hydrologiques, Vol. 41(2)*, pp. 153-170.

Mistry, J.F., Naik, D.M., and Pathak, R.Y. (1984) Estimation of flood discharges by loop rating curves, 51st Annual R&D Session, Central Board of Irrigation and Power, Tech. Sess. II, Paper no. 5, pp. 57-67.

National Weather Service (NWS) (1981) The NWS dam-break flood forecasting model, Users Manual, Davis, Calif. 95616.

Perumal, M. (1994a) Hydrodynamic derivation of a variable parameter Muskingum method: 1. Theory and solution procedure, *Hydrological-Sciences-Journal-des Sciences Hydrologiques, Vol. 39(5)*, pp. 431-442.

Perumal, M. (1994b) Hydrodynamic derivation of a variable parameter Muskingum method: 2.Verification, *Hydrological-Sciences-Journal-des Sciences Hydrologiques, Vol. 39(5)*, pp. 443-458.

Ponce, V.M. (1989) *Engineering hydrology: Principles and practices*, Prentice Hall, Eaglewood Cliffs, New Jersey.

Ponce, V.M. (1991) The kinematic wave controversy, *J. Hydraul. Engg., ASCE, Vol. 117(4)*, pp. 511-525.

Ponce, V.M., and Simons, D.B. (1977) Shallow wave propagation in open channel flow, *J. Hydr. Div.,ASCE, Vol. 103(HY12)*, pp. 1461-1476.

Ponce, V.M., Li, R.M., and Simons, D.B. (1978) Applicability of kinematic and diffusive models, *J. Hydr. Div., ASCE, Vol. 104 (HY3)*, pp. 353-360.

Ponce V.M., A.K. Lohani, and Scheyhing, C. (1996) Analytical verification of Muskingum-Cunge routing, *J. Hydrol., Vol. 174*, pp. 235-241.

Ponce, V.M., Chen, Y.H., and Simons, D.B. (1979) Unconditional stability in convection computation, *J. Hydraul. Div., ASCE, Vol. 105(9)*, pp. 1079-1086.

Price, R.K. (1973) Flood routing methods in British rivers, Proc. Instn. Civil Engrs. (London), Part 2, Vol. 57, pp. 913-930, paper 7674.

Price, R.K. (1985) Flood routing, Ch. 4: *Developments in Hydraulic Engineering*, E.J.P. Novak, Elsevier Applied Science.

Received: 30 October, 1995
Revised: 29 May, 1996
Accepted: 17 June, 1996

Address:
National Institute of Hydrology,
Jal Vigyan Bhawan,
Roorkee 247 667 (U.P.),
India.